SCIENTIFIC REPORTS

OPEN

SUBJECT AREAS:
BIOMATERIALS - PROTEINS
TRANSLATIONAL RESEARCH

Received
23 July 2014

Accepted
13 October 2014

Published
20 November 2014

Correspondence and requests for materials should be addressed to L.W. (katelinwang@gmail.com)

* These authors contributed equally to this work.

Exploring natural silk protein sericin for regenerative medicine: an injectable, photoluminescent, cell-adhesive 3D hydrogel

Zheng Wang[1,2]*, Yeshun Zhang[1]*, Jinxiang Zhang[2], Lei Huang[1], Jia Liu[1], Yongkui Li[1], Guozheng Zhang[4], Subhas C. Kundu[5] & Lin Wang[1,3]

[1]Center for Tissue Engineering and Regenerative Medicine, Union Hospital, Tongji Medical College, Huazhong University of Science and Technology, Wuhan, Hubei China 430022, [2]Department of Surgery, Union Hospital, Tongji Medical College, Huazhong University of Science and Technology, Wuhan, Hubei China 430022, [3]Medical Research Center, Union Hospital, Tongji Medical College, Huazhong University of Science and Technology, Wuhan, Hubei China 430022, [4]The Sericultural Research Institute, Chinese Academy of Agricultural Sciences, Zhenjiang, Jiangsu China 212018, [5]Department of Biotechnology, Indian Institute of Technology, Kharagpur, India 721302.

Sericin, a major component of silk, has a long history of being discarded as a waste during silk processing. The value of sericin for tissue engineering is underestimated and its potential application in regenerative medicine has just begun to be explored. Here we report the successful fabrication and characterization of a covalently-crosslinked 3D pure sericin hydrogel for delivery of cells and drugs. This hydrogel is injectable, permitting its implantation through minimally invasive approaches. Notably, this hydrogel is found to exhibit photoluminescence, enabling bioimaging and *in vivo* tracking. Moreover, this hydrogel system possesses excellent cell-adhesive capability, effectively promoting cell attachment, proliferation and long-term survival of various types of cells. Further, the sericin hydrogel releases bioactive reagents in a sustained manner. Additionally, this hydrogel demonstrates good elasticity, high porosity, and pH-dependent degradation dynamics, which are advantageous for this sericin hydrogel to serve as a delivery vehicle for cells and therapeutic drugs. With all these unique features, it is expected that this sericin hydrogel will have wide utility in the areas of tissue engineering and regenerative medicine.

Silk contains two major protein components, fibroin and sericin. Fibroin fibers are glued together by sericin to form robust cocoons. While fibroin is widely used in textiles, industrial and medical applications[1], sericin has a long history of being discarded as a waste during the degumming process for separating fibroin from sericin[1,2]. Each year estimated 50,000 tons of unutilized sericin was discarded in degumming wastewater worldwide, posing a contamination threat to environment due to the high oxygen demand for sericin degradation[3]. It would be beneficial for economy and environment if this sericin can be fully utilized as a green material.

Sericin is a group of polypeptides comprised of 17–18 types of amino acids[4,5], among which serine, aspartic acid, and glycine are the three most abundant amino acids[4,6]. Sericin was previously reported to elicit an immune response, which was later demonstrated to be triggered when sericin remains physically associated with fibroin[1,7]. Sericin on its own is found to have no immunogenicity and is now utilized in biomedical applications[8,9]. An increasing number of studies have focused on the usefulness of sericin in biomedical applications. Sericin was reported to have diverse biological activities, such as anti-oxidation, anti-bacterium, anti-coagulation and promoting cell growth and differentiation[10–14]. In the field of regenerative medicine, owing to its biodegradability, easy availability, and hydrophilicity with many polar side groups, sericin is mostly copolymerized, crosslinked, or blended with other polymers to form various scaffolds in order to help obtain improved properties for relevant biomedical applications[15–21], such as skin regeneration[17]. Besides being jointly fabricated with other biomaterials, the possibility of using only pure sericin to generate scaffolds has just begun to be explored. Pure sericin 2D films[15,22,23], fragile gels[24] and 3D sponge-like matrices were reported[24,25]. However, sericin used in these studies is extracted through the conventional harsh method involving high heat and alkali, which are known to cause the degradation of sericin[5,26], producing polypeptides with low molecular weights that are physically fragile[26] and

highly soluble, posing a challenge for effective crosslinking. It remains unclear whether the scaffolds generated using sericin with an intact protein profile will possess any unrevealed physical and chemical properties, which might be potentially valuable for tissue engineering applications.

In this work pure sericin with a well-preserved protein profile is extracted from the cocoons of a natural fibroin-deficient mutant silkworm, *Bombyx mori, 185 Nd-s*, which produces silk cocoons containing mainly sericin[27]. When mixed with glutaraldehyde, the extracted sericin is rapidly crosslinked to form an injectable hydrogel. We report for the first time that this sericin hydrogel has a unique photoluminescent feature, which allows bioimaging and *in vivo* tracking. Further, this newly-fabricated sericin hydrogel is naturally cell-adhesive, supporting effective cell proliferation and long-term survival. The mechanical and degradation properties, and drug release profile of this hydrogel are characterized. Our study reveals the suitability of this covalently-crosslinked sericin hydrogel to act as a multifunctional platform for delivery of bioactive molecules (growth factors and therapeutic drugs) and cells for tissue regeneration.

Results and Discussion

Pure sericin is effectively extracted from fibroin-deficient mutant silkworm cocoons. To isolate pure sericin, we took advantage of silkworm genetics. The cocoons of *Bombyx mori, 185 Nd-s*, a fibroin-deficient mutant silkworm strain (see details in Methods) known to produce cocoons mainly containg sericin[27], were used as a sericin source. In agreement with previous reports[6], the sericin isolated by the conventional high heat/alkali method resulted in protein degradation as evidenced by a smear with the vague bands ranging from 25 ~> 200 kDa (Supplementary Fig. S1). In contrast, the sericin solution obtained through the chemically gentle LiBr extraction method (Fig. 1; also see details in Methods) had a well-preserved protein profile with four clearly different bands at the molecular weights (MW), approximately 60 kDa, 100 kDa, 130 kDa, and >250 kDa (Supplementary Fig. S1). The latter three bands were largely consistent with the distinctive bands identified in intact sericin of native silk that was directly isolated from the middle silk gland of the silkworm, *Bombyx mori*[5]. These results indicate that sericin extracted from the mutant cocoons via the LiBr method contains a putatively intact protein profile.

Rapid gelation and injectability of the sericin hydrogel. Although genipin, which is less toxic than glutaraldehyde, is recently used as a crosslinker for generating scaffolds involving sericin[28], it was reported to alter kinetic profiles of carried drugs[29]. Glutaraldehyde was thus employed as the crosslinker in this study. Washing and neutralizing glutaraldehyde with glycine were used to minimize the toxicity resulted from the possible excessive use of glutaraldehyde during hydrogel fabrication. Although the large proteins with approximate MW 200 kDa were still present in the degraded sericin obtained from the conventional high heat/alkali method (Supplementary Fig. S1), they could not be crosslinked to form a hydrogel when mixed with glutaraldehyde even for 7 days. This might be in part because the harsh extraction conditions significantly reduced the amount of amines that would otherwise be available for crosslinking. In contrast, the sericin solution extracted using LiBr was rapidly crosslinked, forming a hydrogel (Fig. 1). This hydrogel was readily cast into various shapes using plastic molds (Fig. 1). Importantly, this soft and flexible hydrogel was injectable (Fig. 1; Supplementary Video S1). The sericin hydrogel could be conveniently injected through the needles with various gauge sizes (Supplementary Video S1), suggesting a possibility of delivering this hydrogel via minimally invasive approaches. To our knowledge, this is the first study reporting the successful fabrication of a covalently-crosslinked, injectable hydrogel using only pure sericin.

We next determined the crosslinking rate of the hydrogels prepared with the different concentrations of sericin. The higher concentration of sericin resulted in faster gelation. 2.6% sericin formed a hydrogel within 23 seconds, while 1.56% sericin took approximately 90 seconds, nearly tripled (Fig. 2a). As the crosslinking degree of polymers affects the degradation dynamics and swelling[30], we next examined the relative crosslinking degree of this sericin hydrogel using the ninhydrin (NHN) assay that is often used to determine free amines in peptides and proteins. The crosslinking degree reached 95% after mixed with glutaraldehyde for 0.5 hour (Fig. 2b). No further increase was observed afterwards. These results indicate that the vast majority of free amines in sercin are rapidly and effectively crosslinked within a short time frame. Given the known types of amino acids in sericin[4], lysine (2.5%) and arginine (3.1%)[4] were likely the two major amino acids donating their amines for crosslinking during gelation. Further, the fast gelation feature may allow the sericin hydrogel to be used in the biomedical applications demanding rapid gelling, such as bleeding prevention that requires the gelation time less than 3 minutes[31].

Porous microstructure of the sericin hydrogel. Porous matrices provide space for cells to proliferate and survive and micro-environment for retention and release of bioactive molecules[32]. In order to obtain the controlled pore size, the sericin hydrogels were frozen at the different temperatures prior to lyophilization. The pore diameters of the lyophilized 3D scaffolds were reduced as the temperature decreased (Fig. 3a; Table 1), which was also observed for the sericin conduits (Fig. 3b and c). The range of the obtained pore diameters (316.9 μm at −20°C, 167.1 μm at −80°C, and

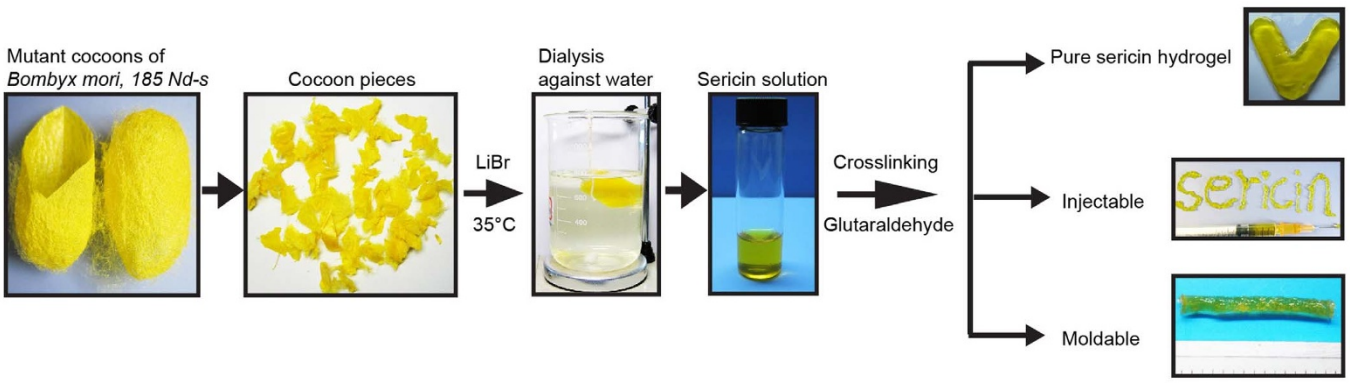

Figure 1 | A flow chart depicts the procedure of extraction, purification and fabrication of a pure sericin 3D hydrogel (details see Methods). Cocoons from a fibroin-deficient mutant silkworm, *Bombyx mori, 185 Nd-s*, were cut into pieces and then dissolved in 6 M LiBr aqueous solution at 35°C for 24 hours. The solution was dialyzed against water for 2 days at room temperature. Glutaraldehyde as a crosslinking agent was added into the sericin solution, leading to the formation of the sericin hydrogels. These sericin hydrogels are injectable and moldable.

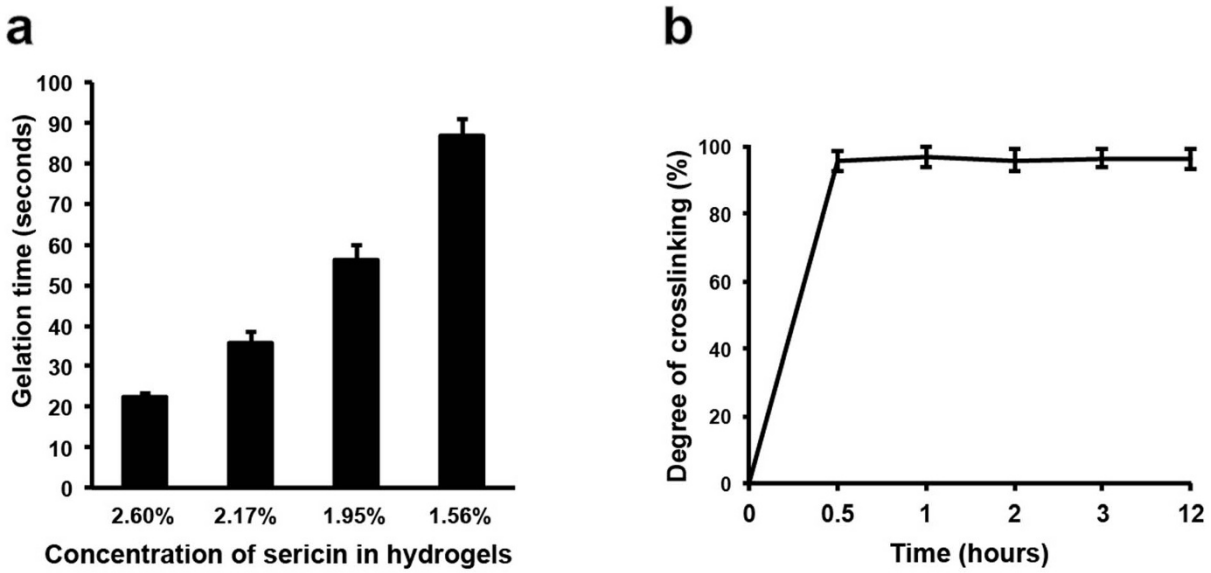

Figure 2 | Gelation dynamics of the sericin hydrogels. (a) Quantification of the gelation time of the sericin hydrogels prepared with the different concentrations at room temperature. (b) Quantification of the crosslinking degree of the sericin hydrogels (2%, w/v) over 12 hours at 37°C.

20.6 μm at −196°C) met the various pore-size requirements for regeneration of multiple different tissues, such as skin (optimal pore size, 20 ∼ 125 μm) and bone (optimal pore size, 100 ∼ 350 μm)[33], suggesting that the sericin hydrogel may be broadly applicable for repair of different types of tissues. Moreover, the porosity of the sericin hydrogels lyophilized at −80°C reached 91.3%. Such high porosity along with the marked interconnectivity among pores would be beneficial for cell seeding and exchange of nutrients and metabolites between seeded cells and *in vivo* microenvironment[34]. Given the significant impact of the hydrogel 3D structure on cell growth and function[35], the microscale features of the sericin hydrogel, including pore sizes, clusters of pores, and

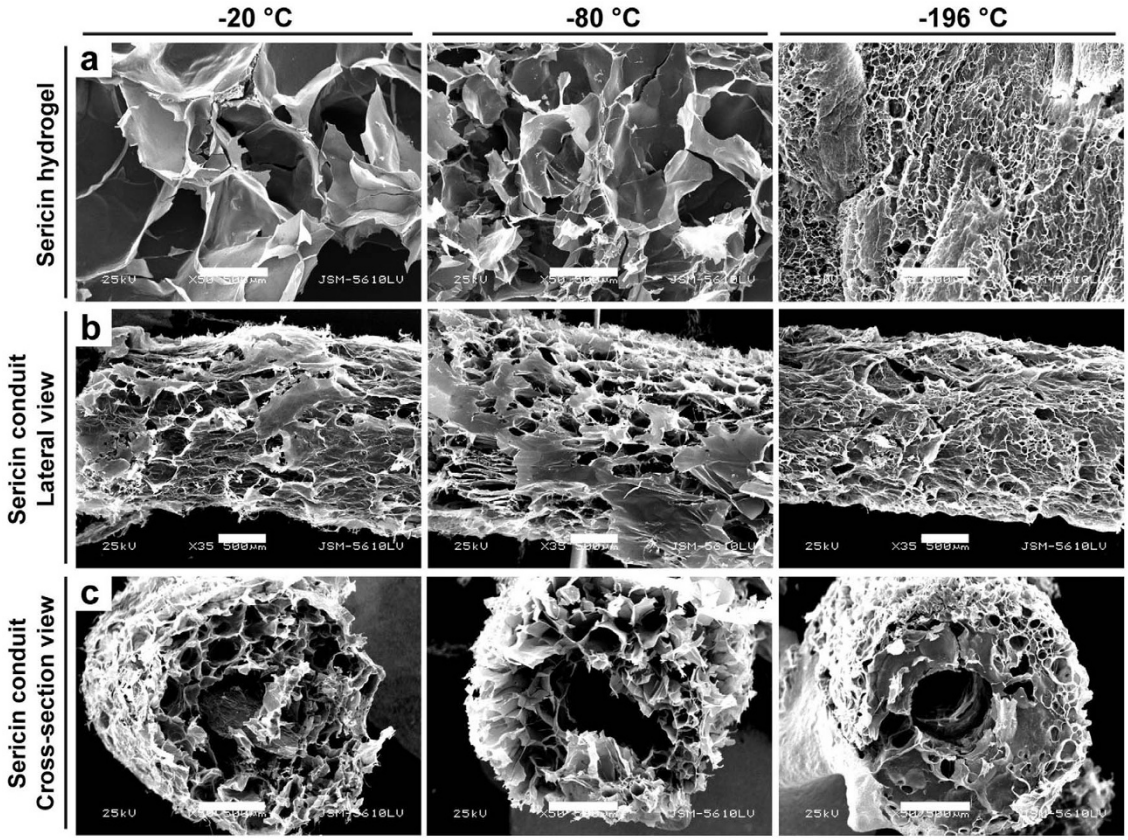

Figure 3 | The porous microstructure of the sericin hydrogels revealed by scanning electron microscopy. (a) The micrographs showed that the random regions of the lyophilized sericin hydrogels frozen at the different temperatures. (b) The longitudinal lateral views of the lyophilized sericin hydrogel conduits. (c) The cross-section views of the lyophilized sericin conduits. Scale bars, 500 μm.

Table 1 | Pore size and porosity of the sericin hydrogels frozen at −20°C, −80°C, and −196°C

Sericin hydrogels [a]	−20°C	−80°C	−196°C
Average pore size (μm)	316.91 ± 45.22	167.13 ± 43.40	20.56 ± 6.43
Porosity (%)	N.D.	91.33 ± 2.20	N.D.

[a]Date shown as mean ± SD (25 random pores per sample, 3 samples for each analysis).
N.D.: not determined.

interconnectivity, may be further designed and/or fine tuned towards the diverse tissue engineering applications through proper techniques, such as gas foaming and electrospinning.

Mechanical characterization of the sericin hydrogel. Porosity can influence mechanical properties, an important feature of a 3D hydrogel[34]. As high porosity may make a hydrogel physically weak, we next sought to determine the mechanical properties of the sericin hydrogel. Since alginate hydrogels were intensively characterized and widely utilized in tissue engineering applications[36], we used 2% and 4% alginate hydrogels as the controls. Given the elasticity of the sericin hydrogel (Supplementary Video S2), we performed the compressive stress-strain analysis. 2% sericin hydrogel showed a 75.77% increase in breaking strain (Table 2) when compared to the alginate hydrogels, suggesting a better compression-bearing capability of the sericin hydrogel. The compressive modulus of the sericin hydrogel (2%) was lying between that of 2% alginate hydrogel and that of 4% alginate hydrogel (Table 2), consistent with the evident elasticity of the sericin hydrogel. These results indicate that the sericin hydrogel has a good compressive mechanical property, providing potential handling convenience during implantation.

FTIR and X-ray diffraction analyses suggest that crosslinking does not cause significant secondary structural transformations. Fourier transform infrared spectroscopy (FTIR) and X-ray diffraction were used to analyze the secondary structure transformations resulted from glutaraldehyde crosslinking. The polypeptide and protein repeat units produce multiple characteristic infrared absorption bands, including amide I, II, and III. Amide I (1600–1690 cm^{-1}) mainly arises from the C=O stretching vibrations of the peptide linkages. Amide II (1480–1575 cm^{-1}) derives from N-H bending and the C-N stretching vibration. Amide III (1229–1301 cm^{-1}) primarily represents C-N stretching vibration linked to in-plane N-H bending vibration. Of these, amide I is the most useful for analyzing sericin protein secondary structures[37,38]. In amide I, the characteristic absorption peaks of β-sheets, random coils, and α-helices are at 1630, 1645, and 1655 cm^{-1}, respectively[22,39,40]. Sericin that we used had a peak of amide I at 1651 cm^{-1} (Supplementary Fig. S2). Since this peak was similarly observed for random coil conformation (1650 cm^{-1}) in native sericin directly extracted from the silk gland of the *Bombyx mori* fibroin-deficient strain "Sericin Hope"[37,38] (see Methods for detailed information), the 1651 cm^{-1} peak we observed likely represented the presence of the random coil structure and α-helix conformation with low-abundant β-sheets. This secondary structure composition was different from that of native sericin extracted from the strain "Sericin Hope", which was rich in both random coils and β-sheets with low-abundant α-helices[37], suggesting that the strain differences influence the secondary structure of sericin. After crosslinking with glutaraldehyde, the amide I peak of the sericin hydrogel slightly shifted to 1655 cm^{-1} (Supplementary Fig. S2), suggesting that glutaraldehyde crosslinking leads to a slight transformation towards α-helix structure and does not cause significant structural transformations.

Crystallinity of the sericin hydrogel was analyzed using X-ray diffraction. Consistent with sericin's characteristic diffraction peaks at 19.2° (2θ) and 23.2° (2θ)[15], our sericin exhibited two diffraction peaks at 19.08° (2θ) and 22.86° (2θ) (Supplementary Fig. S2), which were similar to the two peaks of the sericin hydrogel at 19.02° (2θ) and 23.02° (2θ) (Supplementary Fig. S2). This similarity indicates that glutaraldehyde crosslinking does not significantly increase crystallinity, consistent with the slight difference observed for the amide I peaks of sericin and the crosslinked sericin hydrogel.

The acidic environment constrains the swelling of the sericin hydrogel. Swelling properties of a hydrogel indicate the ability to absorb water, which is crucial as it affects many aspects of a hydrogel, such as diffusion of encapsulated bioactive agents[41,42]. To characterize the swelling behavior of this sericin hydrogel, we examined the swelling process of the lyophilized hydrogel scaffolds in three conditions: acidic, neutral and alkaline. We immersed the hydrogel in PBS with pH adjusted to be 3.0 (acidic), 7.4 (neutral) and 11.0 (alkaline), respectively, at 37°C (Fig. 4a). During the first 3-hour immersion, the volume of the sericin hydrogels increased sharply to 50% of the final maximum swollen volume in all three tested pH conditions. This fast phase was followed by a two-week slow swelling. During the entire process, the swelling rates (increased volume percentage per hour) were similar across all three tested pH conditions. A maximum 26-fold swelling was observed after this two-week immersion at pH 7.4 (neutral) and 11.0 (alkaline). A less swelling, 21 folds, was observed at pH 3 (acidic). These results suggest that the sericin hydrogel has the excellent water absorption capability, which may be in part due to high porosity and hydrophilicity of this hydrogel.

While the swelling rate of the sericin hydrogel was independent of pH conditions, the maximum swelling degree was reduced in the acidic environment. This was due to the chosen acidic pH, which was close to sericin's isoelectric point (pI), approximately pH 4[4]. Under this condition, the polyampholytic sericin hydrogel had zero net charge and the minimal intermolecular repulsive force, which would prevent swelling. As the pH value of the solvent went up, the net charge of the sericin hydrogel turned increasingly negative, which in turn would generate intermolecular repulsive force promoting swelling. Meanwhile, the ionization and hydrophilicity of the sericin hydrogel also increased, favoring swelling[43]. This explains the higher

Table 2 | Mechanical properties of sericin hydrogels and alginate cylindrical hydrogels

Hydrogels[a]	Sericin hydrogel (2%, w/v)	Alginate hydrogel (2%, w/v)	Alginate hydrogel (4%, w/v)
Compressive strength (kPa)	55.539 ± 0.25	38.796 ± 0.448	35.287 ± 0.615
Compressive modulus (kPa)	1.679 ± 0.022	0.644 ± 0.051	6.836 ± 0.291

[a]The hydrogels are 8 mm in thickness and 12 mm in diameter.
Date are shown as mean ± SD (n = 3 for each analysis).

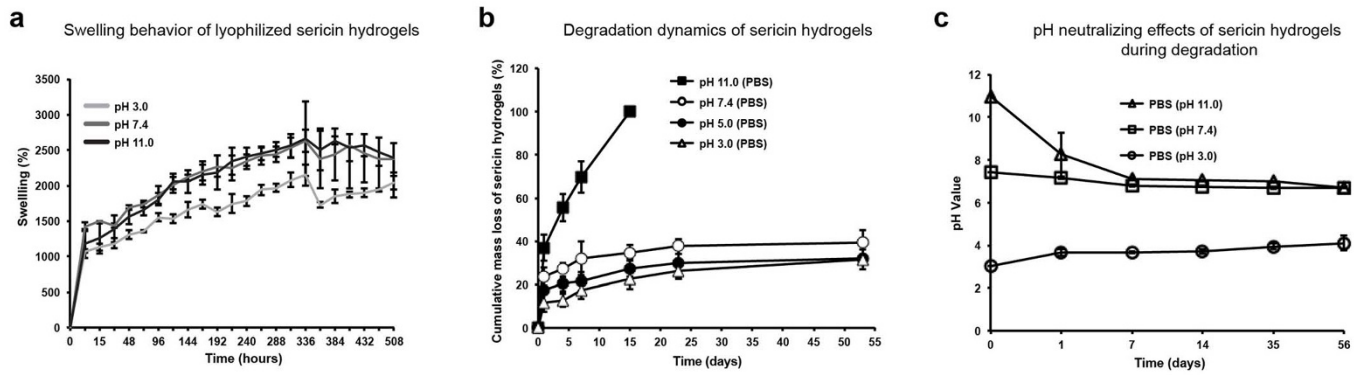

Figure 4 | The swelling behavior and degradation kinetics of the sericin hydrogels. (a) The swelling dynamics of the sericin hydrogels in PBS with different pH (3, 7.4, 11) at 37°C. (b) The degradation kinetics of the sericin hydrogels immersed in PBS with different pH (3.0, 5.0, 7.4, 11.0). (c) The effects of degraded products from the sericin hydrogels on pH of PBS with the different starting pH.

swelling ratio observed for the neutral (pH 7.4) and alkaline (pH 11) conditions. The swelling ratios at pH 7.4 and 11 were similar, possibly because net charge, ionization, and hydrophilicity of the sericin hydrogel were also similar at these two pH conditions. The pH responsive swelling behavior within the acidic-neutral range suggests that the sericin hydrogel may potentially act as a self-regulated carrier for bioactive agents in acidic conditions, such as tumor niche[44].

pH-dependent biodegradability and pH neutralizing effect during sericin hydrogel degradation. Controlled degradation of a hydrogel is important for tissue replacement and drug release, as degradation leaves space for newly regenerated tissue, allows for integration of delivered cells with the surrounding tissues, releases encapsulated bioactive molecules, and avoids the needs for subsequent surgical retrieval of implanted scaffolds. The weight loss resulted from the degradation of the sericin hydrogels was examined in the aqueous conditions with different pH. Given that the content of acidic amino acids (Glu and Asp, 24%) in sericin is higher than that of alkaline amino acids (Lys, His and Arg, 8%)[45], the sericin hydrogel and its degraded products are expected to be slightly acidic. Consistent with this notion, the sericin hydrogels were degraded rapidly and completely within 15 days in the alkaline solution (pH 11.0) (Fig. 4b). In contrast, only approximately 40% of the total amount was lost at pH 3.0, 5.0 and 7.4 after a significantly longer time period (53 days) (Fig. 4b). These results suggest that the alkaline environment results in more effective degradation of the sericin hydrogels than the acidic and neutral conditions. Further, during sericin degradation, the alkalinity of the PBS that was initially adjusted to be pH 11 decreased to a level close to the neutral (Fig. 4c), indicating that the degraded products can neutralize the alkaline aqueous environment, consistent with the expected acidic nature of sericin's degraded products. This pH neutralizing effect might help enhance the stability of the drugs that are unstable in the alkaline condition.

The photoluminescent property of the sericin hydrogel enables in vivo detection and tracking. Photoluminescent materials that allow biological tracking without the aid of extra fluorophores are highly desired[46]. Notably, sericin exhibited intrinsic fluorescence when excited by the light with the wavelengths ranging from 280 nm to 560 nm (Fig. 5a). The emission spectra of the sericin solution fell into two wavelength ranges, 280 nm to 300 nm (with high-intensity peaks), and 340 to 600 nm (with low-intensity peaks) (Fig. 5a). Three aromatic amino acids, tyrosine, phenylalanine and tryptophan, are known to produce intrinsic protein fluorescence[47]. Although the abundance of amino acids is somewhat variable across different reports, the existence of two of those three aromatic amino acids, tyrosine (2.1%) and phenylalanine (0.9%)[4], in sericin partially explained the fluorescence observed. To test whether this intrinsic protein fluorescence could be inherited by the sericin hydrogel, we examined the emission spectra of the sericin hydrogel. The hydrogel emitted fluorescence with the emission spectra falling into two different wavelength ranges, 300 nm to 600 nm (low-intensity peaks), and 500 nm to 700 nm (high-intensity peaks) (Fig. 5a), indicating a red shift in the emission spectra in comparison to the sericin solution. The spectral and intensity features of the intrinsic protein fluorescence are complicated and difficult to predict. These features are influenced by many factors, such as protein tertiary structure/confirmations, spatial distribution of the fluorescent amino acids within proteins, their side chain interactions with other residues or solvent, and resonance energy transfer among those fluorescent amino acids[47,48]. This may account for the differences in fluorescence spectra and intensity observed between the sericin solution and the sericin hydrogel.

As sericin hydrogels' emission spectra covered the excitation and emission wavelengths of commonly used fluorescence proteins and dyes, we next tested whether this optical property would allow *in vivo* detection of the sericin hydrogel. We first examined this under the compound microscope. The sericin hydrogel exhibited photoluminescence when exposed to a variety of wavelengths (Fig. 5b–d). Next, we injected the sericin hydrogel beneath the skin and into the muscle tissue (Fig. 5e). Compared to the alginate scaffolds (as the controls) that are known to be non-photoluminescent, the sericin hydrogels were readily detected and visualized *in vivo* (Fig. 5f–h) although the intensity of the emitted fluorescence reduced as the implantation sites deepened (Fig. 5f–h). These results clearly show that without any fluorescence dye/labeling this sericin hydrogel can be optically detected and tracked *in vivo*, suggesting a possibility of using this hydrogel as a bioimaging probe to visualize targeted sites. Further, given that sericin is a natural biocompatible protein, the hydrogel would avoid the substantial cytotoxicity caused by the organic fluorescent dyes that are commonly used for *in vivo* tracking and visualization[49,50].

The sustained drug release from the sericin hydrogel. A sustained, localized release profile of a growth factor/drug from a hydrogel is often desired towards optimal tissue regeneration. The controlled release avoids a quick loss of growth factors due to their short *in vivo* half-lives when directly injected, and prolongs the therapeutic effects of drugs at targeted sites[51]. To test the release property of this sericin 3D hydrogel, we chose to analyze the release kinetics of a protein enzyme, horseradish peroxidase (HRP) (Fig. 6). Approximately a quarter (28%) of the total amount of HRP was released from the sericin hydrogel within 24 hours. The cumulative release of 50% HRP was observed by Day 3, which was then followed by a 2-week slow, stable release. After the majority of HRP (84%) was released by Day 14, a plateau was reached. The total released HRP was 85% by Day 20. Together, these observations indicate that the sericin

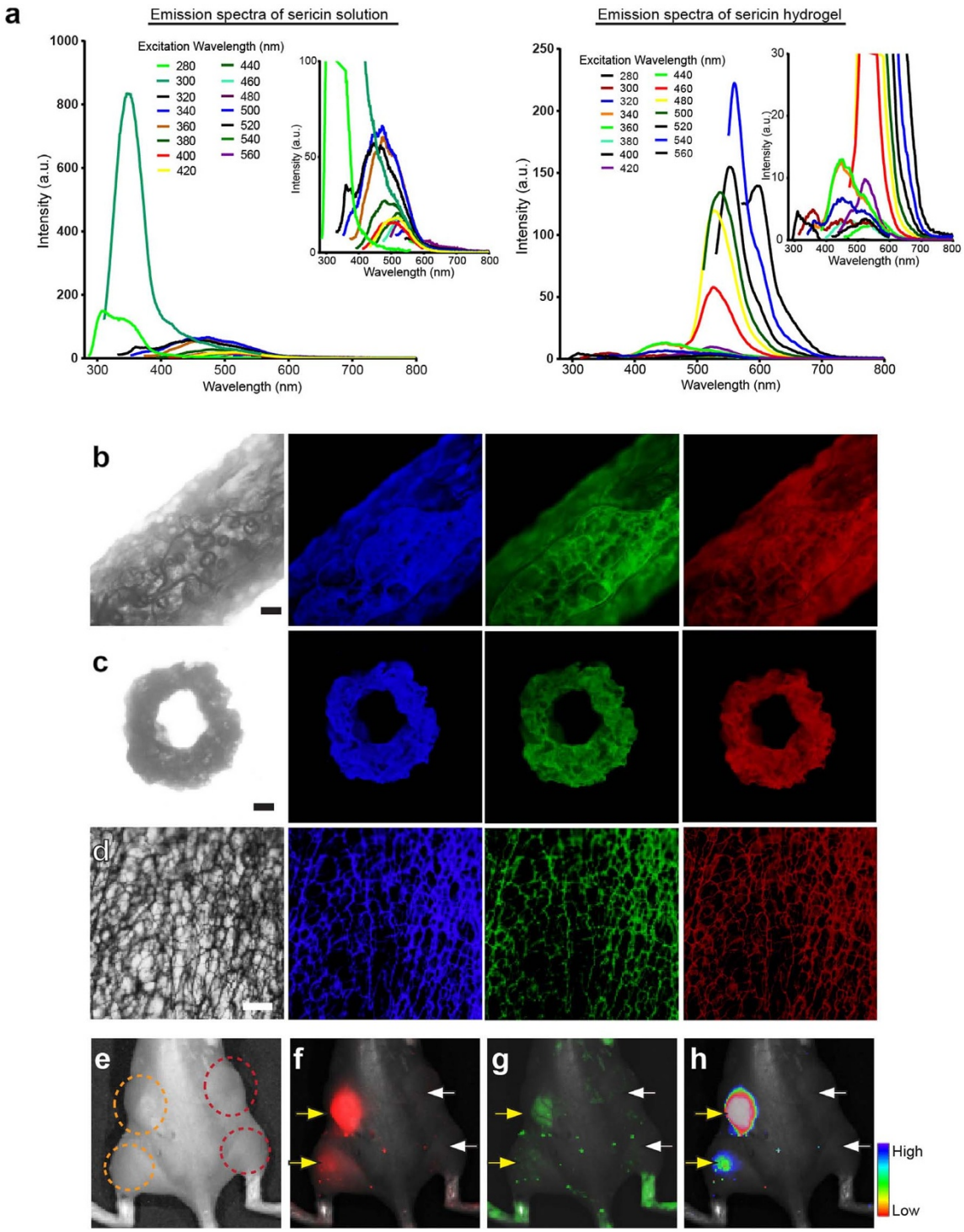

Figure 5 | The photoluminescent property of the sericin hydrogels. (a) The emission spectra of the sericin solution (left) and the sericin hydrogel (right). Each emission spectral curve corresponds to a specific excitation wavelength. The insets showed the enlargement of the low-intensity emission spectra. (b–d) The lateral side of a sericin hydrogel tube (b), the cross-section of this hydrogel tube (c), and the random region of a sericin hydrogel network (d) were imaged under the light at the different wavelengths (left column, imaged under the white light; middle left, imaged with the excitation wavelength 360–370 nm and with the filter allowing the passage of the emission wavelength $>$ 420 nm; middle right, imaged with the excitation wavelength 460–495 nm and with the filter allowing the passage of the emission wavelength $>$ 510 nm; right, imaged with the excitation wavelength 530–550 nm and with the filter allowing the passage of the emission wavelength 575–625 nm). Scale bars, 200 μm. (e–h) *In vivo* light detection of the sericin hydrogels and the alginate scaffolds. (e) The mouse with the sericin hydrogels (outlined with the orange dotted lines) injected subcutaneously to the left back and into the muscle of the left rear limb and the alginate hydrogels (outlined with the dark red dotted lines) injected to the right back and into the muscle of the right rear limb was observed under the bright field. (f) The sericin hydrogels (yellow arrows) were seen under the light at the wavelength 530–550 nm, but the alginate hydrogels (white arrows) were not observed. (g) The sericin hydrogels (yellow arrows) were observed with the light at the wavelength 460–495 nm, but the alginate hydrogels (white arrows) were not seen. (h) The merged image of the bright field and the fluorescent image where fluorescence intensity was represented with a color spectrum.

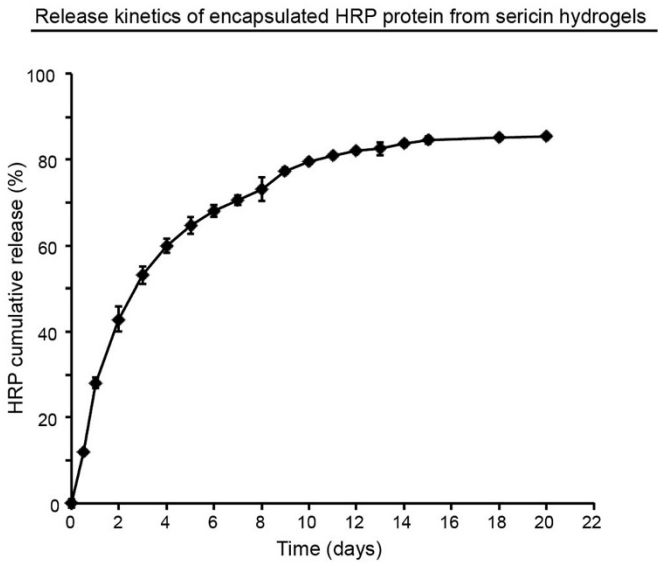

Figure 6 | The sustained drug release kinetics from the sericin hydrogel. The prolonged release of HRP from the sericin hydrogel was observed at 37°C *in vitro* during a period of 22 days.

hydrogel possesses the sustained drug release property, revealing a possibility for this hydrogel to be used as a drug delivery vehicle *in vivo*.

The sericin 3D hydrogel supports effective cell adhesion and growth. The suitability of a 3D hydrogel as a potential cell carrier is largely dependent on its influence on cell behavior. To characterize the effects of this sericin 3D hydrogel on cell behavior, we examined cell adhesion and proliferation, two fundamental cell activities, on this sericin hydrogel with an array of different cell types ranging from epithelial cells, myoblasts to microglial cells (Supplementary Table S1). Once seeded on the sericin hydrogel, the cells started attaching to the hydrogel surface with the adhesion efficiency similar to the cells placed onto the polystyrene surface of culture dishes (Fig. 7a and b). After 24 hours of all the seedings, the attached cells spread on both the hydrogel and the polystyrene surface in a morphologically comparable manner (Fig. 7a). Some types of cells, such as HEK293 (human embryo kidney cells), tended to grow in clusters on the hydrogel surface (Supplementary Fig. S3), suggesting that the sericin hydrogels can influence the spatial distribution of cells. This however appeared to be a cell-type specific phenomenon, as other cell types, such as C2C12 (mouse myoblasts) and HaCaT (human keratinocytes), did not show this distribution pattern. We next examined cell proliferation. The cells examined (Supplementary Table S1) were able to proliferate on the hydrogel surface (Fig. 7a and Supplementary Fig. S4) and continued to grow and survive for up to 20 days (Fig. 7a). Some types of cells, such as human umbilical vein endothelial cells (ECV304), proliferated with a viability rate similar to those on the polystyrene surface (Fig. 7c). To further characterize the impact of the hydrogel on cells, we examined the organization of actin cytoskeleton, which plays a key role in cell adhesion and mobility[52]. The cells growing on the sericin hydrogel developed well-oriented F-actin stress fibers that were visually indistinguishable to those formed by the cells on the culture dish (Fig. 7d), suggesting a potential functional resemblance. These observations indicate that the sericin 3D hydrogel is naturally cell-adhesive and provides a physically and functionally favorable microenvironment for effective cell proliferation and survival. Given the biodegradability and the excellent biocompatibility with an array of different cell types, this sericin hydrogel may act as a degradable extracellular matrix and a temporary cell delivery vehicle to help restore the function and the structure of various injured tissues and organs.

Sericin was reported to enhance attachment of human skin fibroblasts when coated on petri dishes[53]. This was thought to depend on the serine-rich repetitive motif that consists of 38 amino acids and is highly abundant in sericin[53]. Intriguingly, sericin hydrolysates containing this repetitive motif was found to promote cell growth[26] and protect cells from serum-deprivation-induced cell death[54]. Although these observations reflect the excellent biocompatibility of sericin, they might not fully explain cell proliferation/growth observed in the sericin 3D hydrogel. Another contributing factor may be the hydrogel microarchitecture featured with the highly interconnected pore structure, which is expected to facilitate oxygen and nutrient diffusion[34], thereby benefiting cell survival and growth. Thus, the biocompatibility and the microstructure of the sericin hydrogel together account for effective cell proliferation.

Conclusion. Appropriate carrier scaffolds for delivery of cells and drugs play a crucial role in tissue engineering and regenerative medicine. We show for the first time that pure sericin with a well-preserved protein profile can be effectively crosslinked to form a *bona fide* 3D hydrogel suitable for delivering cells and bioactive molecules. Prior to our study, a few attempts were documented for fabricating non-crosslinked pure sericin spongy hydrogels or films using the freeze-thaw technique[55] or ethanol treatment[22,56]. Compared to these non-crosslinking techniques, the covalent crosslinking of sericin has several advantages: (1) the use of crosslinker allows rapid gelation within minutes, in contrast to non-crosslinking techniques requiring much longer gelation time that was often overnight or even days[22,55,56]. (2) By adjusting crosslinking conditions, including sericin concentrations and the amount of crosslinkers, crosslinking degrees can be readily controlled, providing a convenient way to fine-tune some properties that are associated with crosslinking degrees, such as mechanical strength, elasticity, and porosity. Such property tuning would be difficult to be precisely achieved with non-crosslinking techniques. (3) Since crosslinking degrees can be controlled, experimental reproducibility is presumably higher than that of non-crosslinking techniques. (4) Covalent crosslinking offers high structural stability because covalent bonding is stronger and more stable than hydrogen bonding and van der Waals force that are the major forces maintaining the structure of non-crosslinked gels.

We subsequently performed a comprehensive characterization of our pure sericin hydrogel, which reveals the diverse features of this hydrogel. The injectability allows this hydrogel to be implanted through minimally invasive approaches for tissue repair or disease treatment. The photoluminescent property of the hydrogel enables *in vivo* detection and tracking. More importantly, the natural cell-adhesion property of this hydrogel supports effective cell adhesion and long-term survival. In addition to these unique features, the hydrogel possesses multiple physical and chemical advantages. The high elasticity and compressive capability provide handling convenience. The swelling property, high porosity, pH responsive degradation, and the sustained drug release capability are advantageous for this sericin hydrogel to function as a drug delivery vehicle. Depending on the particular types of tissue and their physiological characteristics, the physical and chemical properties of this hydrogel can be further tailored and customized to suit different tissue repair applications. Thus, we conclude that this covalently-crosslinked sericin hydrogel can serve as a multifunctional platform for cell therapy and drug delivery, which could be broadly applied for regeneration of diverse tissues. Finally, this study further reveals the potential value of sericin as a green material.

Methods

Extraction of sericin protein. *Bombyx mori* is a mulberry domestic silkworm strain that has long been used in silk industry[57]. A natural fibroin-deficient mutant silkworm, *Bombyx mori, 185 Nd-s* (obtained from the Sericultural Research Institute, China Academy of Agricultural Sciences, Zhenjiang, Jiangsu, China) produces

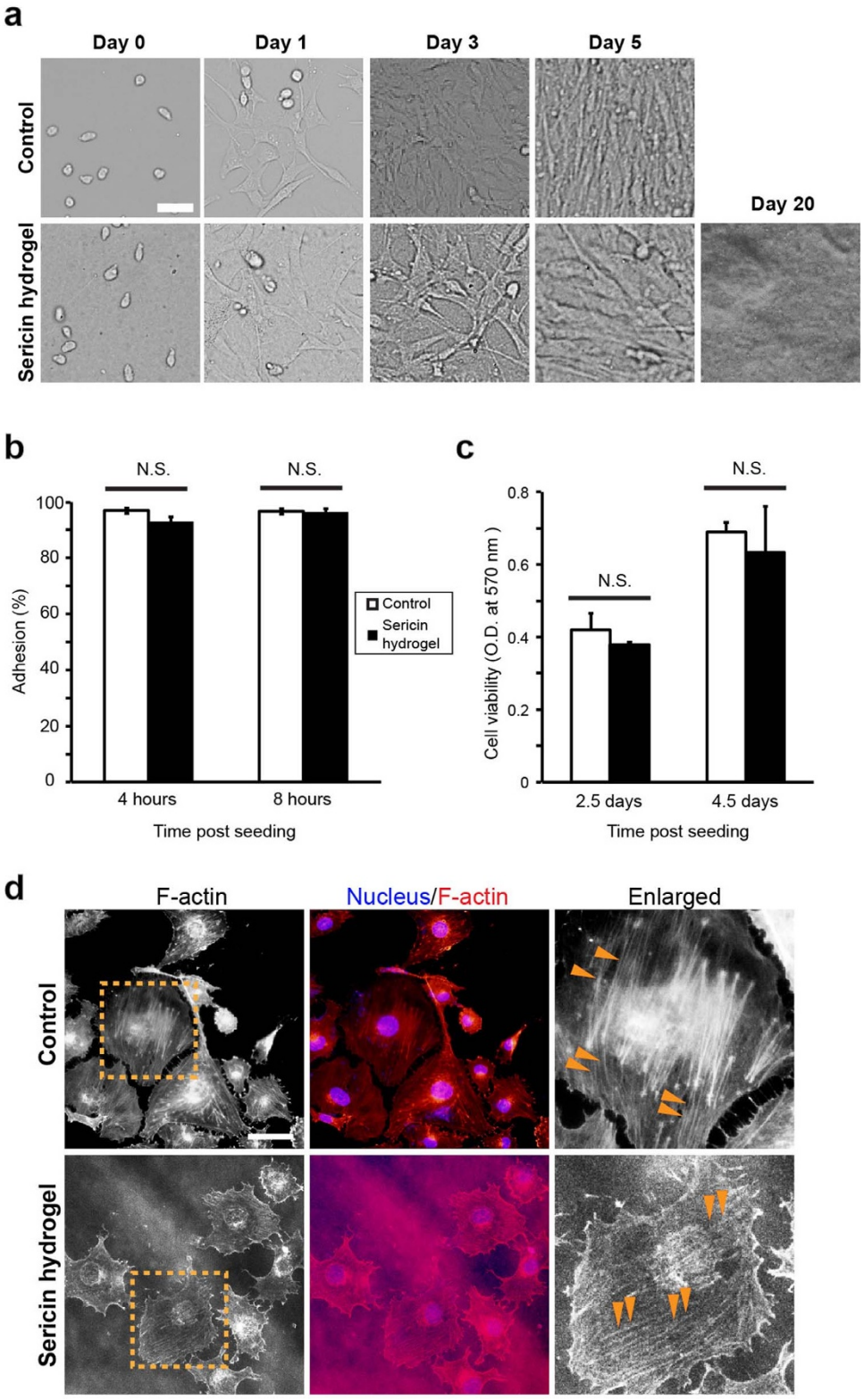

Figure 7 | Cell adhesion and growth on the surface of the sericin hydrogel. (a) The morphology of mouse myoblast cells (C2C12) growing on the polystyrene surface of the culture dishes (upper panel) and the sericin hydrogel (lower panel) at the different time points after seeding. The cells were initially seeded at the density of 5×10^4 per 35-mm culture dish. Scale bars, 50 μm. (b) Quantification of the adhesion of human umbilical vein endothelial cells (ECV304) on the culture dishes and the sericin hydrogel at 4 and 8 hours after seeding. N.S., not significant. (c) The viability of human umbilical vein epithelial cells (EA.hy926) on the culture dishes and on the surface of the sericin hydrogels at Day 2.5 and Day 4.5 after seeding was assessed using the MTT assay and indicated as the O.D. value at 570 nm. (d) Rhodamine-phalloidin staining for F-actin (red) and DAPI staining (blue) for nuclei of ECV304 cells on the culture dishes (upper panel) and the sericin hydrogel (lower panel). The areas outlined by the orange dotted lines were enlarged to show the well-developed F-actin stress fibers (orange arrowheads) in the cells growing on both surfaces. The photoluminescence from the sericin hydrogels resulted in the slightly grainy images. Scale bars, 50 μm.

cocoons that are mainly composed of sericin[27]. *Bombyx mori, 185 Nd-s* was thought to have lower silk spinning frequency than the "Sericin Hope" silkworms, a strain producing sericin only and generated by cross breeding an *Nd* mutant into a high cocoon yielding strain KCS83[58]. The silkworms were bred with fresh mulberry at 25°C. Sericin from the cocoons of *Bombyx mori, 185 Nd-s* was isolated as previously described with modifications[56,59]. Briefly, cut cocoon pieces (1.0 g) were dissolved in 6 M LiBr aqueous solution (55 ml) at 35°C for 24 hours. The insoluble residue was removed by centrifugation and filtration. ¼ (v/v) 1 M Tris-HCl buffer (pH 9.0) was added into the supernatant. This solution was dialyzed (cellulose dialysis membranes, MWCO 3500 Da, Spectrum Laboratory, Inc, USA) against water for 2 days at room temperature. The insoluble residue in the dialyzed sericin solution was discarded by centrifugation. The supernatant was concentrated to the desired concentration using polyethylene glycol (PEG-6000) solution. The obtained sericin solution was kept in refrigerator before use. To determine the molecular weight profiles of the isolated sericin proteins, polyacrylamide gel electrophoresis (SDS-PAGE) was performed as described[5].

Preparation of the sericin hydrogels/scaffolds and quantitative measurement of the gelation kinetics. The sericin hydrogels were prepared from 2% (w/v) sericin solution using glutaraldehyde as the crosslinking agent. At room temperature, 22 μl glutaraldehyde (25%, w/v) was added into 1 ml sericin solution (2%). While the solution was mixed gently, the sericin hydrogels were formed within approximately 60 seconds. The sericin tubes and the other shapes were fabricated by transferring the sericin solutions with glutaraldehyde to the corresponding molds. These prepared samples were repeatedly rinsed with sterilized pure water and treated with 50 mM glycine to neutralize glutaraldehyde. The samples were frozen (at −20°C, −80°C or −196°C for 24 hours) and then subjected to lyophilization. The alginate hydrogels were prepared as the follows: 1 ml 2% (w/v) or 4% alginate solution containing 1 : 1 ratio of high molecular weight (HMW) (FMC Corporation, USA) and low molecular weight alginate (LMW) (obtained from the HMW by gamma irradiation) was mixed with 40 μl $CaSO_4$ (0.21 g/ml) in a syringe[60]. The gelation time was measured as previously described[17]. The gelation time was defined as the time period from when the mixure became viscous to the moment it could not move downwards along the tube wall in the vertically positioned syringe.

Assessment of crosslinking degree. The ninhydrin (NHN) colorimetric assay was used to determine the degree of crosslinking as previously described[61]. The relative percentage of the remaining free amines in the crosslinked sericin hydrogel was calculated. Briefly, the ninhydrin solutions were prepared as follows. Solution A: 0.067 mol/L Na_2HPO_4 (20 ml) was mixed with 0.067 mol/L KH_2PO_4 (5 ml). Solution B: 2 g ninhydrin and 80 mg $SnCl_2$ were added into 5 ml H_2O, stirred for 30 minutes, then stored in a dark bottle for 24 hours. The buffer was then filtered and brought to the volume of 100 ml using water. 100 μl (2%, w/v) sericin solution was mixed with 2.2 μl (25%, w/v) glutaraldehyde; the mixture was then heated to 100°C in water bath with 50 μl solution A and 50 μl solution B for 15 minutes. The solution was cooled down to room temperature. The optical absorbance of the solution at 570 nm was measured with a spectrophotometer (Infinite F50, Tecan, Switzerland). The sericin solutions prepared without glutaraldehyde were used as the controls. The relative degree of crosslinking was calculated using this following equation:

$$\text{Degree of crosslinking } (\%) = \frac{(NH_2)_{nc} - (NH_2)_c}{(NH_2)_{nc}} \times 100 \quad (1)$$

$(NH_2)_{nc}$ and $(NH_2)_c$ are the optical absorbance values that are proportional to free NH_2 in non-crosslinked and crosslinked samples, respectively.

Scanning electron microscopy (SEM) and porosity analysis. The surface of the sericin hydrogel scaffolds was examined under SEM (JSM-5610LV, Japan) with the working voltage 25 kV. The specimens were coated with gold particles with a sputter coater. The pore sizes of the different specimens were averaged from 25 random pores with the Image Pro Plus (version 6.0.0.260). The porosity of the sericin hydrogels were measured by the liquid displacement as previously described[62]. The sericin hydrogels were frozen and then dried by lyophilization. The samples were immersed in the known volume (V_1) of water in a graduated cylinder. After 1-hour immersion, the total volume (including water and the scaffold) was recorded as V_2. The volume of the water remaining in the cylinder after the removal of the scaffold was recorded as V_3. The porosity (ε) of the scaffold was obtained by:

$$\varepsilon(\%) = \frac{v_1 - v_3}{v_2 - v_3} \times 100 \quad (2)$$

Mechanical properties of the sericin hydrogels. A universal testing machine (Instron 5848 MicroTester, USA) equipped with a 100 N load cell at room temperature, was used to measure the mechanical properties of the sericin hydrogels. The sericin hydrogels molded into a cylindrical structure (height 8 mm, diameter 12 mm) were used for tests. The samples were examined at a crosshead speed of 1 mm/min. The alginate hydrogels were used as the controls.

Fourier transform infrared spectroscopy (FTIR) and X-ray diffraction analyses. FTIR spectra of sericin protein and the sericin hydrogel crosslinked by glutararadehyde were acquired using a fourier transform infrared spectroscopy (Nexus, Thermal Nicolet, USA) for the spectral region of 4000–650 cm^{-1} with a ZnSe ATR cell. The X-ray diffraction analysis was performed using the rotation anode high power X-ray diffractometer (D/MAX-RB, Rigaku, Japan).

Analysis of swelling behavior of the sericin hydrogel. The dynamic swelling of the sericin hydrogels was analyzed as previously discribed[17]. The scaffolds were dried, weighed and immersed in PBS (pH 3.0, pH 7.4, pH 11.0). At the different time points, the scaffolds were taken out and the amount of water absorbed was determined by weighing. The swelling ratios of the scaffolds were calculated using the following equation:

$$\text{Swelling } (\%) = \frac{W_s - W_d}{W_d} \times 100 \quad (3)$$

W_s and W_d are swollen weight and dry weight of the sericin hydrogel, respectively.

***In vitro* degradation under different pH environments and the effect of their degradation products on pH.** The sericin hydrogels were incubated at 37°C in PBS with pH adjusted to be 11.0, 7.4, 5.0, 3.0, respectively. The starting concentration of sericin in this solution system was equivalent to 70 mg (sericin dry weight)/ml. PBS was replaced daily. At the different time points, the samples were taken out, dried and weighted. pH of the solution was determined using a pH meter pp-15 (Sartorius, Germany).

Photoluminescent property of the sericin hydrogels. The photoluminescence spectra of the sericin solution and the sericin hydrogel were acquired using an RF-5301 PC fluoro spectrophotometer (Shimadzu, USA). The slit width for the excitation light and the emission light was set to 5 nm and 3 nm, respectively. The fluorescence microscope (Olympus IX71, Japan) equipped with a DP73 camera was used to examine sericin scaffolds under the light with the different wavelengths. The images were taken with the software cellSens standard 1.7 (Olympus, Japan). For *in vivo* real-time tracking analysis, the sericin hydrogels were injected subcutaneously and into the muscle of the rear limbs of Kunming mice at the age of 5 weeks (Department of Experimental Animals, Tongji Medical College, Huazhong University of Science & Technology, Wuhan, China). The alginate scaffolds were used as the controls. Mice were imaged using the Xenogen IVIS Lumina II *in vivo* imaging system with the software Living Image 4.3 (Caliper Life Sciences, USA). All the animal experiments were carried out in accordance with the guidelines evaluated and approved by the Ethics Committee of Huazhong University of Science & Technology (Wuhan, China).

***In vitro* analysis of horseradish peroxidase (HRP) release from the sericin hydrogels.** The drug release from the sericin hydrogels *in vitro* was analyzed using the method previously reported[63]. The HRP loaded sericin hydrogels were prepared by blending 1/125 (v/v) HRP (2 μg/μl) with the sericin solution (2%, w/v). The mixed solution was added into an 48-well plate (500 μl/well). Glutaraldehyde of 11 μl (25%, w/v) was added into each well and mixed well. The samples were left at room temperature for 0.5 hour and stored at 4°C for 24 hours. PBS of 1 ml (pH 7.4) was added into each well. The samples were kept at 37°C. At the different time points, the supernatant from the wells was transferred to a tube. pH of the supernatant was monitored and held constant at 7.4. The HRP content in the withdrawn supernatant was determined by ELISA.

Cell culture on the culture dishes and the sericin hydrogels. Mouse islet endothelial cells (MS-1) were cultured with low glucose DMEM media. Mouse microglial cells (BV2) were cultured using DMEM/F12 media. Human skin epidermal cells (HaCaT) and human primary embryo skin fibroblasts (CCC-ESF-1) were cultured in 1640 media. Mouse myoblasts (C2C12), human embryo kidney cells (HEK293), and human umbilical vein endothelial cell lines (ECV304 and EA.hy926) were cultured with high glucose DMEM. All media contained 10% fetal bovine serum (FBS), 100 units/ml penicillin and 100 μg/ml streptomycin. The cells were cultured in the incubators maintained at 37°C with 5% CO_2 under fully humidified conditions. The culture media was replaced daily. To seed cells onto the hydrogels, the hydrogel was washed by sterilized pure water twice, immersed in fresh PBS (pH 7.4) for 12 hours and then sterilized via immersion in 75% ethanol for 1 hour followed by fresh PBS (pH 7.4) wash 3 times in order to remove alcohol before cell seeding. The cells were harvested from culture dishes, suspended in fresh culture media, and were seeded onto the hydrogels drop by drop. The cell-laden hydrogels were cultured with complete cell culture media at 37°C in a 95% oxygenated tissue culture hood.

Confocal imaging analysis of F-actin stress fibers on the sericin hydrogels. The cell-laden sericin hydrogels were immersed in PBS (pH 7.4) for 10 minutes, removed and fixed by incubating with 4% paraformaldehyde for 10 minutes. The fixed samples were stained with rhodamine-phalloidin to visualize F-actin and 4′, 6-diamidino-2-phenylindole (DAPI) to visualize cell nuclei. The samples were imaged using a confocal laser scanning microscope (Nikon A1Si, Japan).

Cell adhesion and MTT assay. For the cell attachment and MTT assay, the sericin hydrogel was crosslinked, directly formed in the cell culture dishes or the 6-well plates and washed using the same method mentioned earlier in the "Methods" section. Cells were seeded as described above onto the sericin hydrogels or the cell culture dishes (as the controls) and incubated at 37°C. By 4 hours and 8 hours after seeding at the density of 1×10^6 cells per gel, the hydrogel samples were taken out, washed gently

with PBS (pH 7.4). By subtracting the number of the cells washed out by PBS, the number of the cells adhering to each hydrogel was calculated as previsouly described[17]. The MTT assay was employed to assess cell viability at Day 2.5 and Day 4.5 after cells were loaded on the sericin hydrogels in the cell cullture dishes.

Statistical analysis. All data were expressed as mean ± SD. Every sample of each experiment was performed at least three times. Experiments of the MTT assay were run in 6 replicates per test sample. Data were analyzed by ANOVA. Differences between groups of $p \leq 0.05$ were considered statistically significant and those with $p \leq 0.01$ were highly significant.

1. Panilaitis, B. *et al.* Macrophage responses to silk. *Biomaterials* **24**, 3079–3085 (2003).
2. Zhang, Y. Q. Applications of natural silk protein sericin in biomaterials. *Biotechnol Adv* **20**, 91–100 (2002).
3. Aramwit, P., Siritientong, T. & Srichana, T. Potential applications of silk sericin, a natural protein from textile industry by-products. *Waste Manage Res* **30**, 217–224 (2012).
4. Ogino, M. *et al.* Interfacial behavior of fatty-acylated sericin prepared by lipase-catalyzed solid-phase synthesis. *Biosci Biotechnol Biochem* **70**, 66–75 (2006).
5. Takasu, Y., Yamada, H. & Tsubouchi, K. Isolation of three main sericin components from the cocoon of the silkworm, bombyx mori. *Biosci Biotechnol Biochem* **66**, 2715–2718 (2002).
6. Kundu, S. C., Dash, B. C., Dash, R. & Kaplan, D. L. Natural protective glue protein, sericin bioengineered by silkworms: Potential for biomedical and biotechnological applications. *Prog Polym Sci* **33**, 998–1012 (2008).
7. Aramwit, P., Kanokpanont, S., De-Eknamkul, W. & Srichana, T. Monitoring of inflammatory mediators induced by silk sericin. *J Biosci Bioeng* **107**, 556–561 (2009).
8. Zhang, Y. Q. *et al.* Silk sericin-insulin bioconjugates: Synthesis, characterization and biological activity. *J Control Release* **115**, 307–315 (2006).
9. Zhang, Y.-Q., Tao, M.-L., Shen, W.-D., Mao, J.-P. & Chen, Y.-h. Synthesis of silk sericin peptides–l-asparaginase bioconjugates and their characterization. *J Chem Technol Biotechnol* **81**, 136–145 (2006).
10. Baba, T., Hanada, K. & Hashimoto, I. The study of ultraviolet b-induced apoptosis in cultured mouse keratinocytes and in mouse skin. *J Dermatol Sci* **12**, 18–23 (1996).
11. Kato, N. *et al.* Silk protein, sericin, inhibits lipid peroxidation and tyrosinase activity. *Biosci Biotechnol Biochem* **62**, 145–147 (1998).
12. Sasaki, M., Kato, N., Watanabe, H. & Yamada, H. Silk protein, sericin, suppresses colon carcinogenesis induced by 1,2-dimethylhydrazine in mice. *Oncol Rep* **7**, 1049–1052 (2000).
13. Takeuchi, A. *et al.* Heterogeneous nucleation of hydroxyapatite on protein: Structural effect of silk sericin. *J R Soc Interface* **2**, 373–378 (2005).
14. Miyazaki, T. *et al.* Control of bioresorption of porous alpha-tricalcium phosphate by coating with silk sericin. *Trans Mater Res Soc Jpn* **29**, 4 (2004).
15. Nayak, S., Talukdar, S. & Kundu, S. C. Potential of 2d crosslinked sericin membranes with improved biostability for skin tissue engineering. *Cell Tissue Res* **347**, 783–794 (2012).
16. Lim, K. S. *et al.* The influence of silkworm species on cellular interactions with novel pva/silk sericin hydrogels. *Macromol Biosci* **12**, 322–332 (2012).
17. Kundu, B. & Kundu, S. C. Silk sericin/polyacrylamide in situ forming hydrogels for dermal reconstruction. *Biomaterials* **33**, 7456–7467 (2012).
18. Cho, K. Y. *et al.* Preparation of self-assembled silk sericin nanoparticles. *Int J Biol Macromol* **32**, 36–42 (2003).
19. Ahn, J. S., Choi, H. K., Lee, K. H., Nahm, J. H. & Cho, C. S. Novel mucoadhesive polymer prepared by template polymerization of acrylic acid in the presence of silk sericin. *J Appl Polym Sci* **80**, 274–280 (2001).
20. Nagura, M., Ohnishi, R., Gitoh, Y. & Ohkoshi, Y. Structures and physical properties of cross-linked sericin membranes. *J Insect Biotechnol Sericol* **70**, 149–153 (2001).
21. Pushpa, A., Vishnu, B. V. G. & K.S., T. R. Preparation of nano silk sericin based hydrogels from silk industry waste. *J Environ Res Develop* **8**, 243–253 (2013).
22. Teramoto, H., Kameda, T. & Tamada, Y. Preparation of gel gilm from *bombyx mori* silk sericin and its characterization as a wound dressing. *Biosci Biotechnol Biochem* **72**, 3189–3196 (2008).
23. Turbiani, F. R. B., Tomadon, J. J., Seixas, F. L. & Gimenes, M. L. Properties and structure of sericin films: Effect of the crosslinking degree. *Chem Eng Trans* **24**, 1489–1494 (2011).
24. Nishida, A. *et al.* Sustained-release of protein from biodegradable sericin film, gel and sponge. *Int J Pharm* **407**, 44–52 (2011).
25. Nayak, S., Dey, S. & Kundu, S. C. Skin equivalent tissue-engineered construct: Co-cultured fibroblasts/keratinocytes on 3d matrices of sericin hope cocoons. *PLoS ONE* **8**, e74779 (2013).
26. Terada, S., Nishimura, T., Sasaki, M., Yamada, H. & Miki, M. Sericin, a protein derived from silkworms, accelerates the proliferation of several mammalian cell lines including a hybridoma. *Cytotechnology* **40**, 3–12 (2002).
27. Lü, H. S. *et al.* The sericultural science in china:Genetics of the silkworm 1st ed., shanghai scientific and technical publishers. (1990).
28. Aramwit, P., Siritientong, T., Kanokpanont, S. & Srichana, T. Formulation and characterization of silk sericin–pva scaffold crosslinked with genipin. *Int J Biol Macromol* **47**, 668–675 (2010).
29. Thakur, G. *et al.* Crosslinking of gelatin-based drug carriers by genipin induces changes in drug kinetic profiles in vitro. *J Mater Sci Mater Med* **22**, 115–123 (2011).
30. Liang, H. C., Chang, Y., Hsu, C. K., Lee, M. H. & Sung, H. W. Effects of crosslinking degree of an acellular biological tissue on its tissue regeneration pattern. *Biomaterials* **25**, 3541–3552 (2004).
31. Peng, H. T. & Shek, P. N. Development of in situ-forming hydrogels for hemorrhage control. *J Mater Sci Mater Med* **20**, 1753–1762 (2009).
32. Agrawal, C. M. & Ray, R. B. Biodegradable polymeric scaffolds for musculoskeletal tissue engineering. *J Biomed Mater Res* **55**, 141–150 (2001).
33. Whang, K. *et al.* Engineering bone regeneration with bioabsorbable scaffolds with novel microarchitecture. *Tissue Eng* **5**, 35–51 (1999).
34. Annabi, N. *et al.* Controlling the porosity and microarchitecture of hydrogels for tissue engineering. *Tissue Eng Part B Rev* **16**, 371–383 (2010).
35. Khademhosseini, A. & Langer, R. Microengineered hydrogels for tissue engineering. *Biomaterials* **28**, 5087–5092 (2007).
36. Rowley, J. A., Madlambayan, G. & Mooney, D. J. Alginate hydrogels as synthetic extracellular matrix materials. *Biomaterials* **20**, 45–53 (1999).
37. Teramoto, H. & Miyazawa, M. Analysis of structural properties and formation of sericin fiber by infrared spectroscopy. *J Insect Biotechnol Sericol* **72**, 157–162 (2003).
38. Teramoto, H. & Miyazawa, M. Molecular orientation behavior of silk sericin film as revealed by atr infrared spectroscopy. *Biomacromolecules* **6**, 2049–2057 (2005).
39. Jackson, M. & Mantsch, H. H. The use and misuse of ftir spectroscopy in the determination of protein structure. *Crit Rev Biochem Mol Biol* **30**, 95–120 (1995).
40. Jackson, M. & Mantsch, H. H. Protein secondary structure from ft-ir spectroscopy: Correlation with dihedral angles from three-dimensional ramachandran plots. *Can J Chem* **69**, 1639–1642 (1991).
41. Akturk, O. *et al.* Evaluation of sericin/collagen membranes as prospective wound dressing biomaterial. *J Biosci Bioeng* **112**, 279–288 (2011).
42. Smart, J. D. The basics and underlying mechanisms of mucoadhesion. *Adv Drug Deliv Rev* **57**, 1556–1568 (2005).
43. Betz, M., Hormansperger, J., Fuchs, T. & Kulozik, U. Swelling behaviour, charge and mesh size of thermal protein hydrogels as influenced by ph during gelation. *Soft Matter* **8**, 2477–2485 (2012).
44. Justus, C. R., Dong, L. & Yang, L. V. Acidic tumor microenvironment and ph-sensing g protein-coupled receptors. *Front Physiol* **4** (2013).
45. Tao, W., Li, M. & Xie, R. Preparation and structure of porous silk sericin materials. *Macromol Mater Eng* **290**, 188–194 (2005).
46. Yan, X., Li, J. & Mohwald, H. Templating assembly of multifunctional hybrid colloidal spheres. *Adv Mater* **24**, 2663–2667 (2012).
47. *Principles of fluorescence spectroscopy* (ed JosephR Lakowicz) Ch. 16, 529–575 (Springer US, 2006).
48. Eftink, M. in *Topics in fluorescence spectroscopy* Vol. 6 *Topics in fluorescence spectroscopy* (ed JosephR Lakowicz) Ch. 1, 1–15 (New York, Springer US, 2000).
49. Gao, X. *et al.* In vivo molecular and cellular imaging with quantum dots. *Curr Opin Biotechnol* **16**, 63–72 (2005).
50. Jamieson, T. *et al.* Biological applications of quantum dots. *Biomaterials* **28**, 4717–4732 (2007).
51. Chen, R. R. & Mooney, D. J. Polymeric growth factor delivery strategies for tissue engineering. *Pharm Res* **20**, 1103–1112 (2003).
52. Tojkander, S., Gateva, G. & Lappalainen, P. Actin stress fibers--assembly, dynamics and biological roles. *J Cell Sci* **125**, 1855–1864 (2012).
53. Tsubouchi, K., Igarashi, Y., Takasu, Y. & Yamada, H. Sericin enhances attachment of cultured human skin fibroblasts. *Biosci Biotechnol Biochem* **69**, 403–405 (2005).
54. Takahashi, M., Tsujimoto, K., Yamada, H., Takagi, H. & Nakamori, S. The silk protein, sericin, protects against cell death caused by acute serum deprivation in insect cell culture. *Biotechnol Lett* **25**, 1805–1809 (2003).
55. Zhang, H. P. *et al.* Preparation and characterization of a novel spongy hydrogel from aqueous bombyx mori sericin. *E-Polymers* (2008).
56. Teramoto, H., Nakajima, K. & Takabayashi, C. Preparation of elastic silk sericin hydrogel. *Biosci Biotechnol Biochem* **69**, 845–847 (2005).
57. Xia, Q. *et al.* Complete resequencing of 40 genomes reveals domestication events and genes in silkworm (bombyx). *Science* **326**, 433–436 (2009).
58. Mase, K., Iizuka, T., Okada, E., Miyajima, T. & Yamamoto, T. A new silkworm race for sericin production, “sericin hope” and its product, “virgin sericin&rdquo. *J Insect Biotechnol Sericol* **75**, 85–88 (2006).
59. Teramoto, H., Nakajima, K.-i. & Takabayashi, C. Chemical modification of silk sericin in lithium chloride/dimethyl sulfoxide solvent with 4-cyanophenyl isocyanate. *Biomacromolecules* **5**, 1392–1398 (2004).
60. Wang, L., Shansky, J., Borselli, C., Mooney, D. & Vandenburgh, H. Design and fabrication of a biodegradable, covalently crosslinked shape-memory alginate scaffold for cell and growth factor delivery. *Tissue Eng Part A* **18**, 2000–2007 (2012).
61. Yuan, Y. *et al.* The effect of cross-linking of chitosan microspheres with genipin on protein release. *Carbohydr Polym* **68**, 561–567 (2007).
62. Mandal, B. B., Priya, A. S. & Kundu, S. C. Novel silk sericin/gelatin 3-d scaffolds and 2-d films: Fabrication and characterization for potential tissue engineering applications. *Acta Biomater* **5**, 3007–3020 (2009).

63. Wang, X. *et al.* Silk coatings on plga and alginate microspheres for protein delivery. *Biomaterials* **28**, 4161–4169 (2007).

Acknowledgments

The work is supported by the Recruitment Program of Global Young Experts, the National Natural Science Foundation of China Program 81272559, the International Science and Technology Corporation Program of Chinese Ministry of Science and Technology S2014ZR0340, and the Science and Technology Program of Chinese Ministry of Education 113044A.

Author contributions

Z.W. and L.W. wrote the manuscript. Experiments were designed by L.W., Y.Z., Z.W., L.H., J.L. and Y.L. Y.Z., L.H. and J.Z. performed experiments. Z.W., L.W., Y.Z. and J.Z. analyzed and interpreted data. S.C.K. provided constructive comments on manuscript writing. G.Z. provided cocoons.

Additional information

Supplementary information accompanies this paper at http://www.nature.com/scientificreports

Competing financial interests: The authors declare no competing financial interests.

How to cite this article: Wang, Z. *et al.* Exploring natural silk protein sericin for regenerative medicine: an injectable, photoluminescent, cell-adhesive 3D hydrogel. *Sci. Rep.* **4**, 7064; DOI:10.1038/srep07064 (2014).